Received: 6 December 2021 | Revised: 20 April 2022 | Accepted: 28 May 2022

DOI: 10.1002/rob.22104

RESEARCH ARTICLE

WILEY

Application of automated and robotically deployed in situ X-ray fluorescence analysis for nuclear waste management

Samuel R. White | Peter G. Martin | David A. Megson-Smith | Thomas B. Scott

School of Physics, University of Bristol, Bristol, UK

Correspondence
Samuel R. White, School of Physics, University of Bristol, Tyndall Ave, Bristol BS8 1TL, UK.
Email: sam.white@bristol.ac.uk

Funding information
National Centre for Nuclear Robotics (NCNR); Robotics and AI in Nuclear (RAIN); Engineering and Physical Sciences Research Council; National Nuclear User Facility Hot Robotics (NNUF-HR)

Abstract

Laboratory and synchrotron X-ray fluorescence (XRF) analysis has both served as mainstay rapid and quantitative elemental analysis techniques for decades, attaining parts per million sensitivities for the majority of elements. Formerly, XRF was the reserve of large X-ray generating systems and national facilities. More recently, developments in miniaturized X-ray generators and detectors have allowed for this nondestructive technique to be utilized for portable and in situ elemental characterization of materials, away from the confines of the laboratory. When combined with a robotic manipulator, these usually handheld systems present a powerful method for autonomous assessments of material composition for a wide range of nuclear characterization and decommissioning scenarios. In this study, we present a proof-of-concept XRF system integrated with a robotic manipulator to autonomously identify a suite of nuclear relevant materials. Such remotely deployable noncontact tools are crucial for use within hazardous environments where it may not be possible, for physical and safety reasons, for a human operator to manually undertake characterization tasks. It is envisaged that this robotically deployed XRF system will comprise part of the wider autonomous characterization "toolkit"; capable of extensive large-area mapping alongside targeted compositional "point analysis." The system was demonstrated to rapidly and repeatably derive accurate and precise compositional information of different test materials, autonomously on both flat and complex, object-rich surfaces.

KEYWORDS
characterization, elemental mapping, manipulator, nuclear, robotic assay, robotic vision, X-ray fluorescence

1 | INTRODUCTION

Accurate, precise, and rapid materials characterization is a highly desirable capability in numerous different industrial settings. Applications such as hazardous waste management (Nuclear Decommissioning Authority: Waste Package Specification and Guidance Documentation, 2020), forensics (Zieba-Palus et al., 2008), environmental science (Croudace et al., 2019), and scrap metal assaying (Balasubramanian & Muthukumaraswamy, 2016) are all key examples. While many materials and components are readily discernible, by virtue of their color, luster, and

Equally contributing authors.

geometrical form, other materials are more difficult to differentiate. In particular, metals, alloys, and corroded/coated objects may appear visually identical, but possess different elemental compositions. Such compositional differences can greatly influence how the material should be subsequently handled or managed. Within the nuclear sector, a deployable, in situ, and real-time materials analysis capability is highly desired for use as part of waste management operations (Sellafield Ltd., 2020). In such environments, it is crucial to accurately assay items and consign them to the correct and most appropriate onward processing, recycling, and/or disposal route.

In-field assay techniques are essential to accurately and quantitatively determine elemental composition and distribution within objects, surfaces, and components. However, readily portable assay techniques have historically been very limited. Many lab-based techniques are unsuitable for application on-site, in situ, and in real-time. This has necessitated material subsampling and recovery for laboratory analysis. For direct analysis of solids, scanning electron microscopy, combined with energy dispersive (X-ray) spectroscopy (EDS) is a widely utilized technique for elemental analysis (Girão et al., 2017). Alternatively, inductively coupled plasma mass spectrometry, which requires acid digestion of samples, is widely used to provide the isotopic analysis (Godfrey & Glass, 2011). Whilst they provide high-sensitivity, precision analysis, they are expensive in terms of the high cost of both instrument operation and upkeep (Wilkinson et al., 2011; Wilschefski & Baxter, 2019). In addition, they are expensive with respect to the time taken to extract, handle and ship the samples to the laboratory, as well as the analysis reporting time. Therefore, reducing or eliminating the need for sampling can deliver major cost savings for numerous different nuclear waste management and decommissioning scenarios. Accordingly, nondestructive in situ measurement is highly preferable to facilitate radiological, chemical, and material characterization. In situ analysis can derive almost instantaneous results, whereas subsampling for laboratory analysis may take several days or weeks to complete, slowing down waste management processes and activities. An example of an in situ analysis technique is laser-induced breakdown spectroscopy (LIBS) combined with Raman spectroscopy. These techniques represent highly complementary characterization methods (Muhammed Shameem et al., 2020). While LRS is excellent at characterizing plastics and other chemically bonded materials, it is ineffective at metals analysis. LIBS can identify metals, but the plasma's produced could represent a fire risk, though this is noted as being unlikely (Cremersand & Radziemski, 2006). In addition, the generation of aerosols and airborne particulates may be an issue when used in hazardous environments (Cremersand & Radziemski, 2006). An alternative, nondestructive, in situ analysis technique for metals analysis is X-ray fluorescence (XRF).

1.1 | X-ray fluorescence

XRF is a well-known and widely adopted characterization technique used to nondestructively analyze materials (Streli et al., 1999). As a methodology, it is able to quantitatively ascertain elemental compositions with parts per million (ppm) sensitivities for elements between sodium and uranium. The methodology operates using the principle of X-ray-induced fluorescence; whereby incident X-ray photons are directed onto the sample, resulting in the ionization of the materials constituent atoms. Vacancies are left where electrons have been excited into higher energy states. These resultant vacancies leave the atom in a short-lived unstable state, with electrons from higher-energy orbitals rapidly infilling the vacancies—emitting X-rays of characteristic energies as a result. As each element possesses characteristic fluorescence emission energies, it is these that together contribute to the resultant fluorescence spectra (Callcott, 1999).

The technique requires the simultaneous generation of an incident beam of X-rays; combined with a detection system through which to quantify the fluorescence spectra. Historically, the generation of sufficient X-ray fluences for rapid quantifiable XRF analysis was the preserve of large-scale synchrotron sources and subsequently, advanced high-power and nonportable, laboratory sources (Janssens et al., 2000). However, recent advancements in microelectronics, high-voltage systems, source cooling, and X-ray generators have facilitated the development and production of "handheld" energy dispersive XRF (ED-XRF) with portable instrumentation. These such systems will be referred to herein as simply ED-XRF. They can be operated "in the field" by nonexpert users away from the laboratory, with comparatively low operational costs (Janssens et al., 2013).

Developments in X-ray tube technology have greatly enhanced handheld ED-XRF, as devices which previously relied upon radioisotope excitation now operate using tube-based systems (Thomsen & Schatzlein, 2002). Complimentary to this is the development of Silicon Drift Detectors (SDDs) which enable X-ray detection on a solid-state chip-set using Peltier cooling, rather than needing cumbersome liquid nitrogen cooled detectors, such as those required for more classical silicon and high purity germanium detectors (Longoni et al., 1998). Resultantly, these ED-XRF devices are now widely used across research (Turner, 2017; Turner et al., 2017; Turner & Taylor, 2018), with one of the most common use cases being geological field investigations, whereby rocks and minerals are characterized rapidly and in real-time. In addition, scrap metals merchants increasingly utilize handheld ED-XRF to determine the elemental composition and hence values of metallic articles.

Through XRF point analysis, surfaces can be mapped by making many measurements in a defined pattern, thereby yielding an elemental concentration map, referred to herein as an "XRF map." Perhaps the most notable example of an XRF point analysis system is the Perseverance Rover's Planetary Instrument for X-ray Lithochemistry (PIXL; Allwood et al., 2021). PIXL was mounted on the Rover's robot arm and was capable of high accuracy XRF point analysis of collected samples. Campos et al. (2019) presented a portable XRF mapping system, whereby a 3-axis stage mount with an attached X-ray source and detector was used and moved across a 35 cm × 35 cm scan area. Using a point sampling method, the X-ray source and

detector collected XRF data at multiple locations. This demonstrated a capability to create highly accurate elemental maps—noting discrete chemical changes. The system reported high spatial accuracy, with an elemental map resolution of 1.4 mm. However, the inability to alter the projection angle restricted its ability to scan unusual shapes, such as curved surfaces. Another system offering an XRF mapping capability is the Zetium XRF, produced by Malvern Panalytical (2020). The Zetium system consists of a bench-top machine that offers XRF mapping with a measurement step size of 100 μm. One major limitation of this setup is that it is not capable of analyzing larger, meter-scale objects, which may be required for an in situ analysis technique.

A critical feature for in situ analysis for nuclear materials is that ED-XRF can be deployed as a noncontact analysis technique, thereby avoiding potential pickup of contamination. However, the technique does require a close proximity to a sample surface (0–30 mm), which presents a technical challenge for remote deployments—to get very close, but not so close that contact is made.

1.2 | Manipulator robotics

Over the past decades, robotic manipulators have become commonplace in manufacturing and are extensively used across industrial sectors from aircraft manufacturing (*Tech briefs: Robots bring airplane production up to speed*, 2021) to cake decorating (*FANUC: Robotics in food processing*, 2021). Such robotic systems are currently replacing and augmenting the human workforce. A number of commercially available robotic arms exist, such as those produced by KUKA, FANUC, ABB, and Kinova; demonstrating high levels of repeatability and submillimeter positional accuracy. This makes them excellent platforms for tasks involving repeated motions and precise positioning. Away from their more conventional usage, White et al. (2020) demonstrated the fusion of robotic manipulators with radiation sensors to detect and map the locations of gamma-ray emitting objects distributed across the surface of a sorting table for nuclear applications. In complementary work, Coffey et al. (2021) presented the feasibility study of using coincident LIBS and Raman systems mounted on a robotic arm to successfully compositionally characterize assorted objects contaminated with beryllium. Sensors used by robotic manipulators in this way offer high spatial accuracy and precision compositional characterization. They are also remotely operable in environments which are considered too dangerous or undesirable to send humans, as is the case for many nuclear and/or radiological scenarios.

As already described, there are a number of shortfalls in current laboratory XRF mapping techniques. These limitations include the limited sample sizes that can be accommodated, the requirement to transport samples to the laboratory to subsequently install them within the enclosed instrument, as well as the inability to scan surfaces which are not flat. One methodology to negate such limitations is the application of robotic manipulators paired with ED-XRF devices.

A robotic manipulator system fitted with an ED-XRF device has enormous potential for addressing many of the current ED-XRF mapping limitations. Owing to the large range of processes that such systems currently undertake, robotic manipulators exist in a wide variety of sizes. Many feature a reach of greater than 2 m, thereby facilitating ED-XRF mapping over centimeter to meter length scales. A unique feature of robotic manipulators is their ability to rotate the end flange, known as the "end-effector," to different orientations. This functions very much like the human wrist, while maintaining a high level of spatial and angular precision of the robotic system. Rotational action in this way provides the system with the ability to deploy the ED-XRF unit to derive maps of surfaces with curved or highly varied topology, by keeping the instrument at the appropriate close stand-off distance and perpendicular to the surface. The versatility of robotic manipulators enables them to be combined with additional sensory inputs, such as vision-based technologies, enabling manipulators to move dynamically based on camera feedback. Such a vision-based system could be implemented to increase the efficiency of a process by negating the need to blindly scan across a whole table, instead of targeting only the objects of interest and without coming into physical contact. Modern "collaborative" robotic manipulators even feature force–torque sensing capabilities. These force–torque sensors enable the arm to sense its surroundings, making them human safe. Such an arm could be used here to act as a secondary fail-safe against an unintended collision, reducing damage, and contamination risks.

1.3 | Characterization challenges in nuclear

There are an extensive number of nuclear applications where a robotically operated, rapid, nondestructive, and high-sensitivity quantitative elemental analysis would deliver a step-change in characterization capability. One advantage of a robotic XRF system is the potential for remote or autonomous operation. This could serve to improve worker safety via radiation dose reduction, as well as allowing for analysis to be undertaken within environments where it is not currently possible or practical. The focal point of this study relates to waste sorting and subsequent management processes.

Owing to the rapidly increasing number of nuclear reactors entering the end of their operational lifetimes and subsequently transitioning to decommissioning, there is an ever-growing global drive towards autonomously identifying and sorting mixed wastes. For nuclear decommissioning, it is a required process ahead of packaging and consignment to safe, long-term storage. This characterization process is known as "sorting and segregation" and seeks to assay mixed provenance wastes such as fuel-element debris (FED), aluminum, steel, plastics, and general construction materials to direct them for the most appropriate onward processing and/or disposal stream (Sellafield Ltd., 2020). While approaches and requirements differ somewhat between nations, the classification and segregation of wastes is managed and performed as defined by a

country's designated waste hierarchies and waste types (Wilson, 1996).

This volume of current and "future arisings" of waste exists on top of the backdrop of pre-existing large volumes of mixed legacy wastes held within interim storage facilities at numerous sites around the world. While more modern plants are designed to minimize the volumes and inventories of radioactive waste and additionally streamline end-of-life decommissioning, legacy facilities were not built with this consideration. This has resulted in substantial volumes of assorted wastes; much of which is held in underground storage "vaults" and/or sealed drums awaiting sorting, conditioning, and consigning to final disposal (*Nuclear Decommissioning Authority: Radioactive Waste Strategy*, 2019). It is therefore crucial to understand, to a high level of compositional accuracy, the individual contents of the retrieved mixed wastes to facilitate the consigning of the items to different appropriate waste streams. Efficient and correct sorting is important to protect against expensive wrongful assignations of material, especially materials that have recycle value or could behave problematically in stored wastes (Fujiwara et al., 2017; Nuclear Decommissioning Authority: *Geological Disposal Waste Package Evolution Status Report*, 2016). ED-XRF mapping across a sorting and segregation table could be used to characterize reactive metals and other similarly recyclable materials, ahead of disposal. Waste on a table presents an automation challenge for ED-XRF, as it contains features that may be spread across a large surface on the order of 1–5 m^2.

Ultimately, this waste is destined for storage in waste containers, which themselves must be periodically monitored (Design, 2016). For example, the UK's intermediate-level waste (ILW) inventory comprises some 40,000 stainless steel drums containing grouted wastes. The structural integrity of these drums must be maintained and checked to avoid a radiological release. If the container surface is contaminated with an aggressive species, such as chloride salt, then pitting corrosion may ultimately cause the failure of the container (Nuclear Decommissioning Authority: Waste Package Specification And Guidance Documentation, 2008). In the UK, the Nuclear Decommissioning Authority has stringent guidance on monitoring nuclear waste drums in storage (Nuclear Decommissioning Authority: Waste Package Specification and Guidance Documentation, 2020). Currently, the drums are monitored for chlorides using remotely deployed contact techniques, such as swabbing, tape lifting, or direct flushing of the surface (Nuclear Decommissioning Authority: *Industry Guidance Interim Storage of Higher Activity Waste Packages—Integrated Approach*, 2012). The arising samples all require transporting to a laboratory for analysis, which creates a delay in discerning the outcome of the monitoring and introduces complexity. Noncontact ED-XRF scanning using a robotic manipulator represents a valuable in situ analysis technique for assessing the concentration and distribution of such salts on container surfaces. Hence, the opportunity to provide such analysis in situ and in real-time is highly desirable for nuclear waste storage sites worldwide.

Ostensibly, any radioisotopes which may be present within scanning objectives in a nuclear setting, may themselves introduce X-rays. These X-rays will be recorded as a fluorescence and consequently, skew the results. It is anticipated that the only problematic isotope would be from the americium-241 (Am-241) 60 keV gamma-ray (Kim et al., 2019). This may coincide with the characteristic X-rays of tungsten, rhenium, and potentially lutetium. Although, it is unlikely that there would be a sufficient gamma-ray emission flux from Am-241 to cause such a statistical anomaly. However, it should be advised that a secondary gamma spectroscopy check is undertaken should any of the aforementioned elements arise via XRF analysis.

While the focus of this study is the development of a nuclear-applicable manipulator-integrated ED-XRF system, such a fusion could also be applied more widely; for example, to municipal waste processing or recycling facilities. In electrical waste recycling scenarios, components containing toxic chemicals including lead, cadmium, mercury, and beryllium (Callcott, 1999), may be distributed across a sorting table, awaiting material characterization to provide a safe, environmentally conscious disposal route.

2 | EXPERIMENTAL METHOD

2.1 | X-ray characterization

The combined X-ray generation and fluorescence analysis instrument utilized within this study was the Vanta C-Series ED-XRF from Olympus Corporation (*Olympus Vanta specifications*, 2021). The device is lightweight (1.70 kg with battery) and compact (8.3 cm × 28.9 cm × 12 cm when the optional integrated device handle is removed). A 4 W (50 kV) X-ray tube combined with a silver anode target yields an excitation X-ray source energy of range 8–50 kV. Resulting from the characteristic X-ray emissions of the different elements occurring across the full 8–50 keV energy range, a "three-beam" mode is used whereby three specific beam energies are used to enhance the sensitivities for groups of elements best achieved by that ionization energy. These energies can be tailored to the specific elemental compositions likely to be encountered. The detection of the X-ray-induced fluorescence is performed by the Vanta using an integrated SDD, with the device capable of operating under wide temperature ranges of −10°C to 50°C, enabled by the integrated cooling fan installed next to the SDD module. The mobile unit possesses an Ingress Protection (IP) rating of IP55, meaning it is protected against dust and low-pressure water jets. Therefore, it is well suited for use within contaminated and hazardous environments where material "pick-up" and subsequent decontamination are of concern.

For more routine, manual deployments, the Vanta is typically used in the "gun" configuration, for performing single spot/point compositional assays by hand. Quantitative results can be displayed in real-time on the instruments integrated touch-screen. However, the device is also an ideal detector for robotic research and deployment owing to its programmable operation. Hence, rather than relying on a user to manually initiate each analysis event, it is

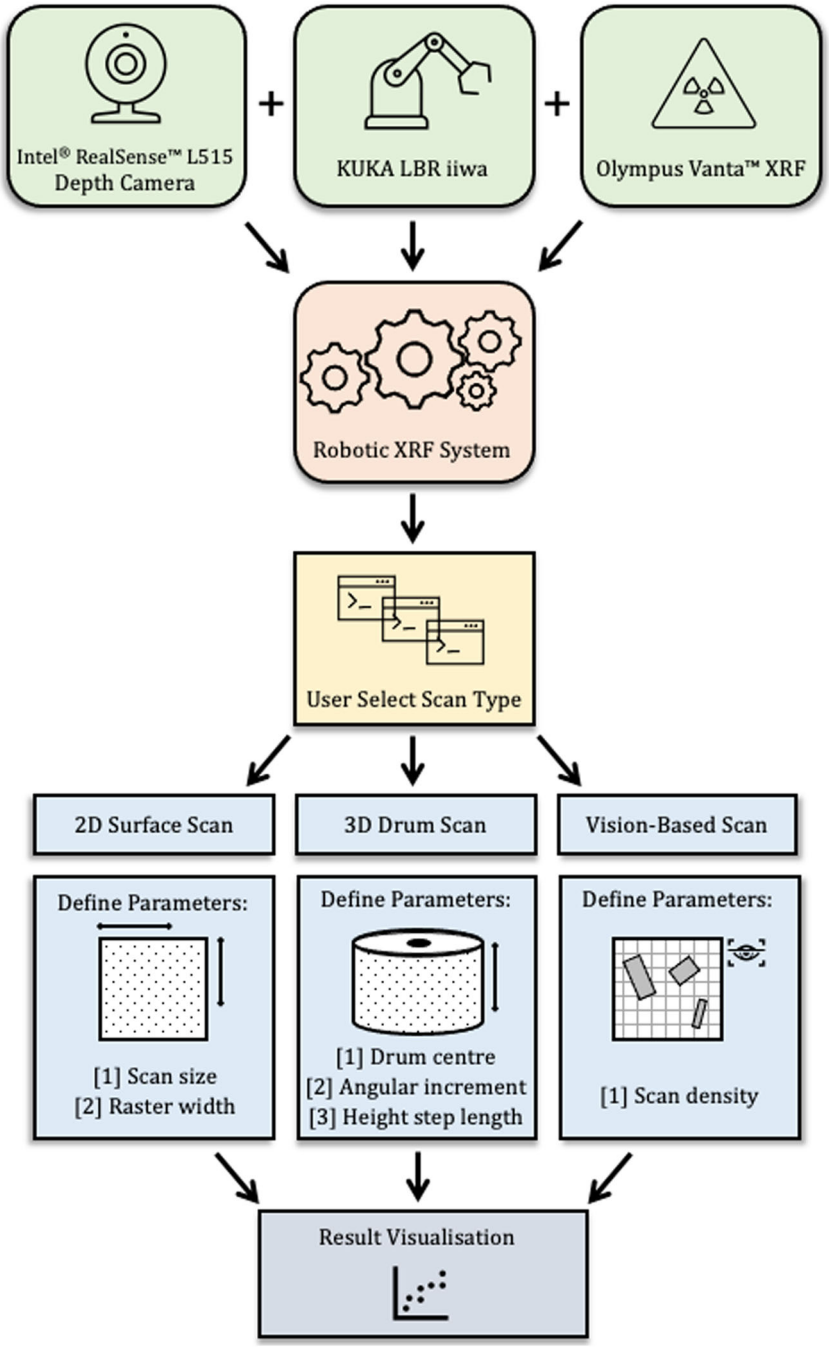

FIGURE 1 Schematic flowchart illustrating the platforms configuration and workflow, including details of the application-specific user parameters necessary to undertake each scanning scenario. 2D, two dimensional; 3D, three dimensional; XRF, X-ray fluorescence.

possible, through the USB-serial connection using a dedicated Linux (Python) software package, to enable X-ray analysis to be triggered remotely. In addition, the Vanta parses both the spectral and peak fitted elemental data (including the necessary analysis errors) directly to the tethered computer, where it can be subsequently processed using custom-designed software developed in this study.

2.2 | Robotic manipulator

The KUKA LBR iiwa R820 (*Kuka lbr iiwa*, 2021) was selected for these nuclear-applicable scanning applications. It has an IP rating of 54, being resistant to dust and splashes of water. This makes it suitable for use in an active environment, avoiding the potential undesired ingress of contamination. The arm has a maximum reach of 820 mm and is lightweight at 29.5 kg, allowing it to be transported and easily moved for different applications. Crucially, it is a collaborative arm with force–torque sensors in six of its seven joints. These can be used for collision protection, thus ensuring minimal damage is attained from any accidental contacts. In this study, the Vanta analyzer was attached to the end effector of the robotic manipulator, using an adjustable and configurable sensor rack. This rack could accommodate a range of other sensory options, such as a depth-sensing camera or tactile probe. Before each of the subsequently detailed

applications, a tool center point (TCP) calibration was performed, using the KUKA XYZ four-point method. This method entails orientating the "tool piece" around a defined center point in four different directions. A transformation can then be generated, locating the instrument relative to the end effector.

A custom control software was developed in Python to synchronize the Vanta and KUKA LBR iiwa. The robotic ED-XRF system was programmed to sequentially move through a set of situationally dependent, pregenerated scan positions and pause while ED-XRF data were acquired. Acquisition of ED-XRF data was set for 10 s on beams 1 and 2, with 20 s on beam 3, for all measurements. A set of control parameters were customizable, enabling the user to fine-tune the robotic movements and data collection, including the point density and scan surface type. The point density was configured according to the time available for the scan and dependent on the level of detail that was required. The scan surface type enabled the robotic system to interrogate a choice of flat surfaces or curved surfaces. The location and orientation of the ED-XRF scan head was recorded for each measurement relative to the robotic manipulator, constituting the collection of an $[x, y, z]$ and $[a, b, c]$ coordinate, where $[x, y, z]$ represents the position in free space relative to a predefined base, and $[a, b, c]$ represent Tait-Bryan angles of the ED-XRF module. When the arm was in position, the Vanta was triggered and the ED-XRF data collected.

The collected results, including elemental concentration and associated errors, were recorded in a comma-separated value file. They could then be graphed as an XRF "map" of elemental mass fraction, as part of a visualization software that was developed. Each visualization was bespoke to the scenario for which it was applied and the results could be plotted as discrete, raw values in space both in 2D and 3D. A flowchart detailing the system setup and workflows is shown in Figure 1.

Figure 1 shows the versatility of the system, demonstrating how it may be set up for multiple different applications, including flat surface scanning, waste drum monitoring, and individual object assay.

2.3 | Assessing the quality of concentration results

Operation in a stand-off configuration is not recommended by Olympus. Hence, to validate the precision of the concentration values obtained by the ED-XRF mapping system, a series of paint solutions doped with known quantities of cesium chloride (CsCl) was analyzed as part of a calibration activity. Equal portions of paint (2 ml) were doped with CsCl masses ranging from 0.0 to 3.0 g, in increments of 0.5 g. A strip was produced containing these varying concentrations of CsCl. The robotic ED-XRF system was programmed to perform a line transect scan across the strip, collecting data at 2 mm intervals. A 5-mm stand-off distance was used for the full line transect. The experimental results from the robotic system were then compared with the results from a laboratory bench-top Octane plus EDS (EDAX Inc.). This was completed to ensure that the data derived from the ED-XRF was sufficiently well calibrated.

2.4 | Assorted object assay

In nuclear waste sorting and segregation activities, mixed objects may be randomly distributed across a sorting table, including contaminated pipe work, tools, and rubble (Sellafield Ltd., 2020). Such objects are consigned to their appropriate waste-stream/disposal route based on their radiation level as well as their chemical composition, ensuring that objects are directed to the correct disposal pathway. The objects will need to be assayed to assess their elemental compositions ensuring that the waste can be stored with confidence. For this process, scanning across the whole analysis area would be time consuming and contain many data points where no objects are located on the sorting table. Hence, a robotic vision-based procedure was implemented, using a computer-vision "region-of-interest" methodology. A depth camera was used to identify the objects of interest and consequently inform the robotic ED-XRF system of specific intelligent scan locations to perform ED-XRF. By implementing an intelligent scanning methodology, scanning time can be reduced, while increasing elemental information about objects of interest through a targeted "denser scan" of the nonbackground material.

To achieve this object-targeted scanning, an Intel RealSense L515 depth camera (*Realsense l515 specifications*, 2021) was used in combination with the robotic ED-XRF mapping system to derive an XRF map. The robotic ED-XRF system autonomously moved to an initial camera pose, where it took a depth photo of the scene. This depth image could then be compared with a reference image of the scan area. The resulting depth comparison image reveals positional information about the objects on the surface. A height and area threshold was applied to the comparison image to locate the objects of interest, in this case programmed as 625 connected pixels

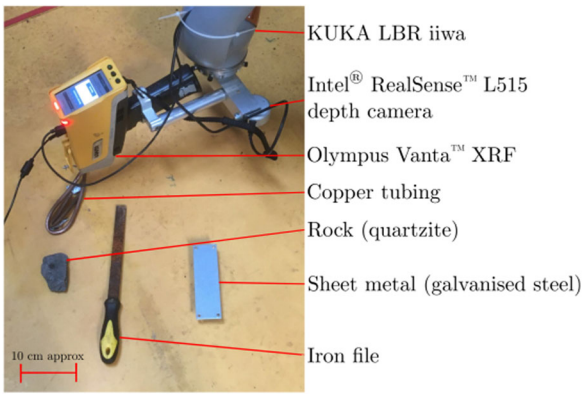

FIGURE 2 Photograph of the vision-based scanning system in progress; showing the assorted objects on the scan surface, the KUKA LBR iiwa, Intel RealSense L515, and Olympus Vanta. XRF, X-ray fluorescence.

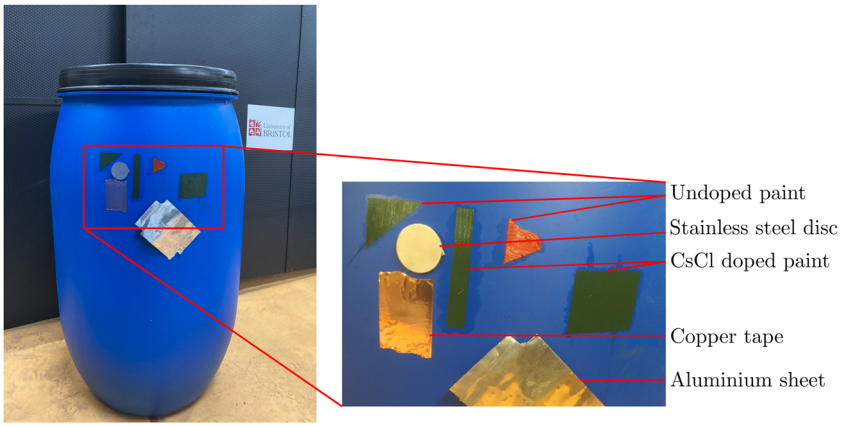

FIGURE 3 Photograph of the drum setup, detailing the positions of the copper tape, CsCl doped paint, undoped paint, aluminum sheet, and stainless steel disc

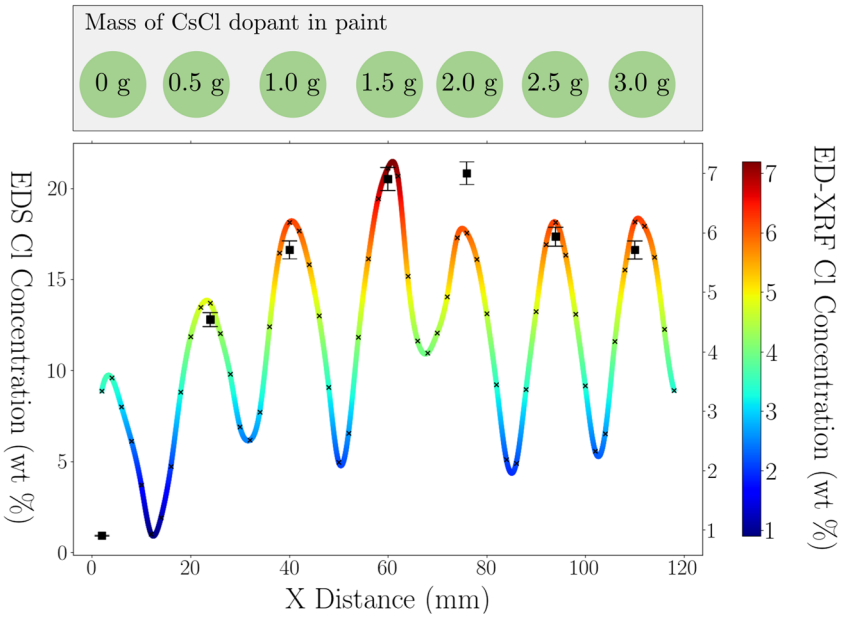

FIGURE 4 Concentration profile of the ED-XRF line scan over a linear transect of the CsCl doped paint. Left to right, the mass of dopant added to the paint was 0.0, 0.5, 1.0, 1.5, 2.0, 2.5, and 3.0 g. The colorful line is an interpolated concentration wt% for Cl along the transect. The black squares represent the results of the laboratory EDS testing, with an associated error. EDS, energy dispersive spectroscopy; ED-XRF, energy dispersive XRF; XRF, X-ray fluorescence.

(approximately 0.04% of the image) for an area-of-interest and 20 mm for object height. This thresholding process identified the pixels of interest from the depth image. It was noted that the edges of objects contained the largest depth uncertainties. Therefore, to reduce such edge effects, an erosion algorithm was used to reduce the area of each identified object. An affine transformation was then applied to convert pixel space into ED-XRF system coordinate space. The robotic ED-XRF system could then scan the autonomously thresholded coordinate points.

Measurements were taken at a predefined stand-off distance from the sample. The stand-off distance has a large effect on the relative concentration of elements within each scan. Therefore, a positional accuracy test was completed on a flat metallic object, where the system was set to scan 50 points at a 15-mm stand-off. A metallic object was selected, as the reflectivity of such surfaces was noted to introduce the largest errors to the system. The test revealed a standard deviation of 2 mm with a range of 10 mm. To be conservative, an error of ±8 mm was assumed, owing to this being the maximal divergence from the true value.

The ED-XRF module itself emits a pencil beam with a small divergence. The geometric specifics of the system are patent protected, but working at a 30-mm stand-off distance, the calculated beam divergence diameter is 11 mm. At a stand-off of 5 mm, the beam divergence diameter is just 2 mm. The error in positional accuracy in the horizontal plane, from the calibration, was found to be 10 mm. Hence, an effective spot size of 21 mm diameter was assumed for the purposes of this study. The primary objective of the system is to quantify the elemental composition of large objects through multipoint analysis. Therefore, such errors were deemed acceptable.

This camera-based algorithm enables the intelligent "region-of-interest" mapping of objects. To test this procedure, two scenarios were prepared using a mock-up waste sorting table of dimension, 300 mm × 600 mm. The first attempted region-of-interest-based mapping of three rectangular metal blocks containing aluminum (Al), copper (Cu), and silumin (an alloy containing Al and silicon). As all samples were flat in profile, a stand-off distance of 5 mm was programmed for this initial test. In the second test, a

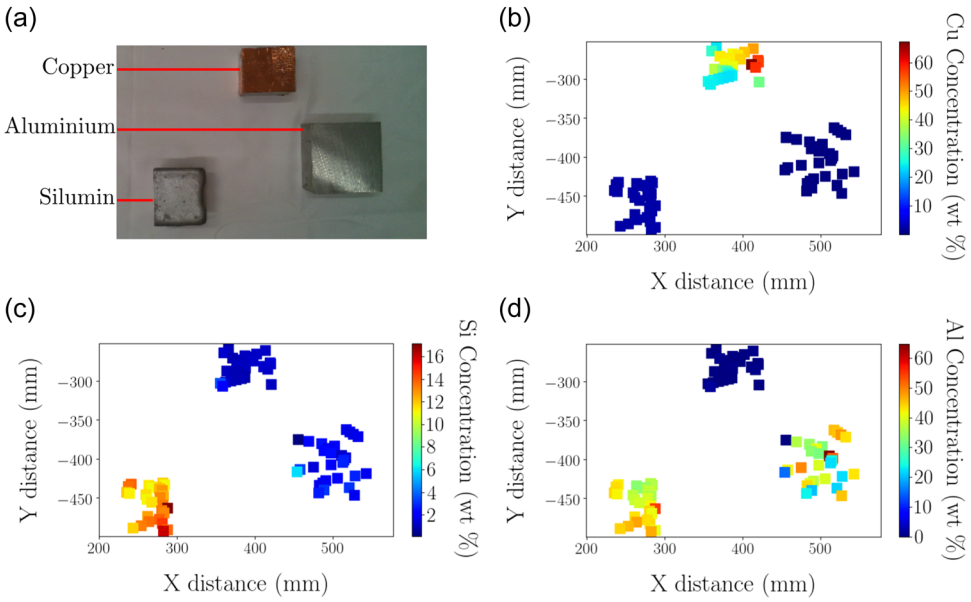

FIGURE 5 Results of the vision-based autonomous robotic ED-XRF mapping of the system identified objects of interest for the metallic block experiment. (a) The experimental setup. The elemental concentrations of (b) Cu, (c) Si, and (d) Al. ED-XRF, energy dispersive X-ray fluorescence.

metal file (Fe), a rock (quartzite), copper tubing (Cu), and a small piece of galvanized steel sheet (Zn) were placed on the mock-up waste sorting table. These objects were selected as they are examples of potential materials which may appear in nuclear waste (Sellafield Ltd., 2020). Owing to the physical dimension of the ED-XRF, a stand-off distance of 20 mm was programmed for this test. This stand-off was selected to ensure the ED-XRF did not make contact with the objects of nonuniform height. Figure 2 shows the object placement and the robotic ED-XRF system scanning in progress.

2.5 | Exterior drum scanning

Orientation control provides the robot-integrated ED-XRF system with a unique capability to compositionally analyze curved surfaces. This ability was tested by performing an area scan on a region of a 220-L plastic drum. When the center point and radius of the curved object (e.g., a drum) relative to a manipulator are known, it is possible to numerically plan a series of equispaced points which traverse an arc via a number of geometrical calculations. By inputting the center point and radius of the drum into the custom scanning control code, point locations were identified including manipulator positions, the ED-XRF scan locations, and TCP orientations. Each position ensured that the ED-XRF device was always directed towards the center of the drum, normal to its surface. The robotic ED-XRF mapping system was then able to obtain elemental composition measurements at each such point. The precise point locations were based on the additional predefined user input parameters. Point density was defined as a function of angular increments on each arc and vertical height step lengths. Using the 3D implementation of the developed plotting software, a surface map of the drum with elemental concentrations was generated. This was tested with different elements applied to the surface including copper tape (Cu), undoped paint, paint doped with cesium chloride (CsCl), an aluminum sheet (Al), and a stainless steel disc (Fe), as shown in Figure 3. The arm was set to scan for approximately 10 h, at 1° increment around a 60° portion of the circumference of the drum, with 10 mm vertical height steps. Measurements were taken from a stand-off distance of between 10 and 25 mm, owing to irregularities in the drum's circumference.

3 | RESULTS AND DISCUSSION

3.1 | Concentration calibration

The results of the concentration line scan test are shown in Figure 4.

Figure 4 demonstrates that it is possible for the robotic ED-XRF system to not only detect certain elements, in this case Cl, but also derive relative concentrations. The results output from the robotic ED-XRF system is proportionally in good agreement with the bench-top EDS setup. However, the ED-XRF results show a large reduction in attained concentration. This is likely a result of a reduced X-ray flux being received by the system, due to the stand-off configuration. A capability to discern approximate weighted concentrations using this system could be particularly useful for applications where there are threshold limits on the concentration

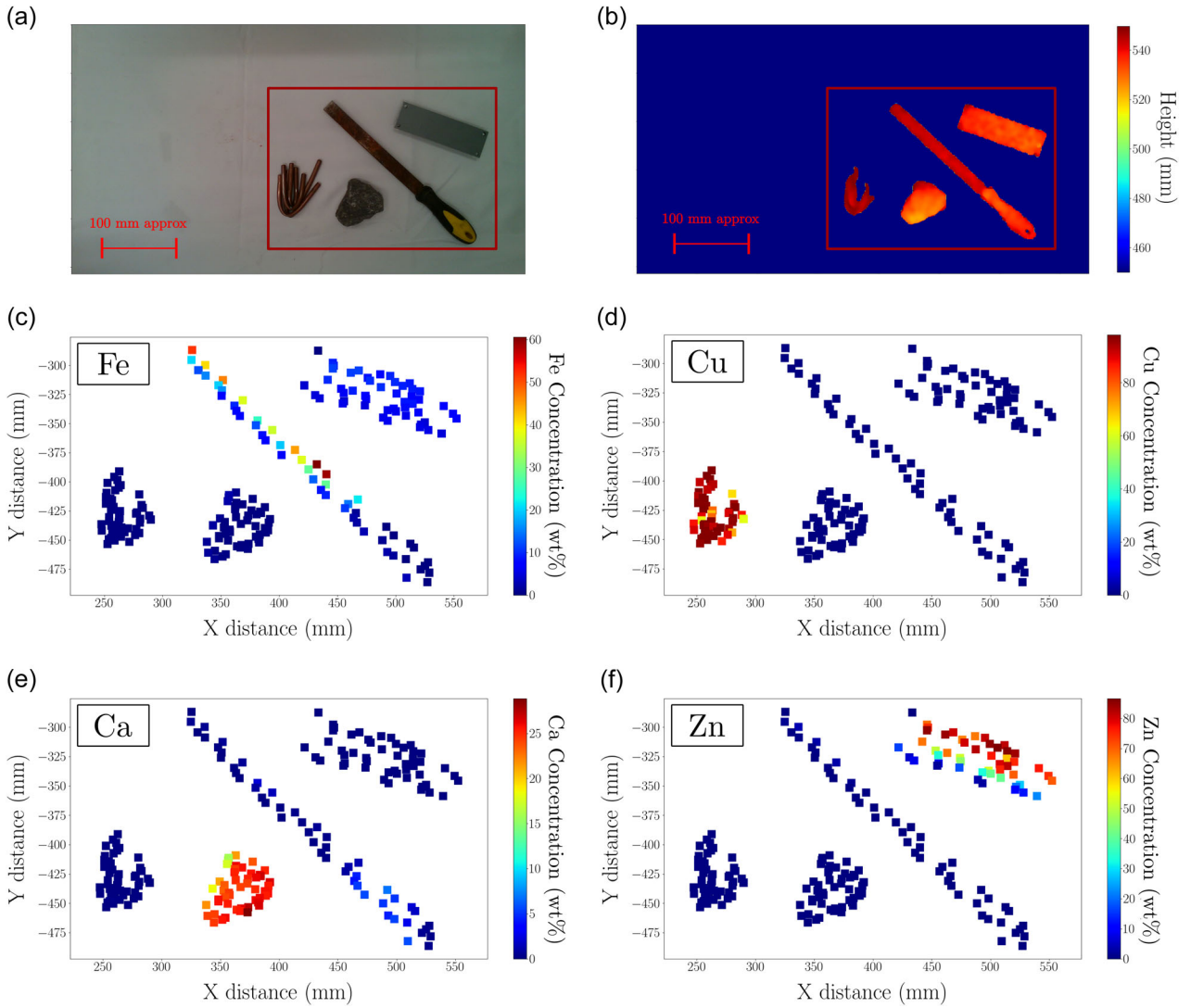

FIGURE 6 Results of the vision-based autonomous robotic ED-XRF mapping of the system identified objects of interest, as shown in Figure 2. (a) Initial photograph from the RealSense L515 camera, (b) depth camera image of (a). The red box in (a) and (b) indicates the region which is displayed in the subfigures, showing the single element XRF maps of (c) Fe, (d) Cu, (e) Ca, and (f) Zn.

of certain compounds. One prominent example of this is the search for chlorides on the exterior of stainless steel ILW drums, where acceptance levels for such contamination are in place for species, such as Cl (see Section 1.3.).

3.2 | Assorted object scanning for sorting

The result of the vision-based scan of the metallic block object scanning experiment is shown in Figure 5.

The results show a good agreement with the true metallic species used for experimentation, correctly identifying the elements within each block. In addition, this experiment confirms the vision-based region-of-interest algorithm functions, as expected. All blocks scanned were of the same height, hence analysis of stand-off distance could be completed. The results showed that an average stand-off of 10 mm was recorded across the data set, with a standard deviation of 2 mm. These results were greater than anticipated, but within the tolerance of the system. A more representative example of a waste sorting scenario was completed in a second experiment, the results of which can be seen in Figure 6.

The assimilation of camera-based object identification subsequently delivers targeted ED-XRF elemental analysis with each object identified by the vision-based XRF scan. The results represent a powerful result and methodology for object assay, facilitating the characterization of individual objects. Whilst caution should be exercised in attributing quantitative analysis to the elemental concentrations, the system is able to accurately identify the key elements present. All of the objects were scanned in approximately

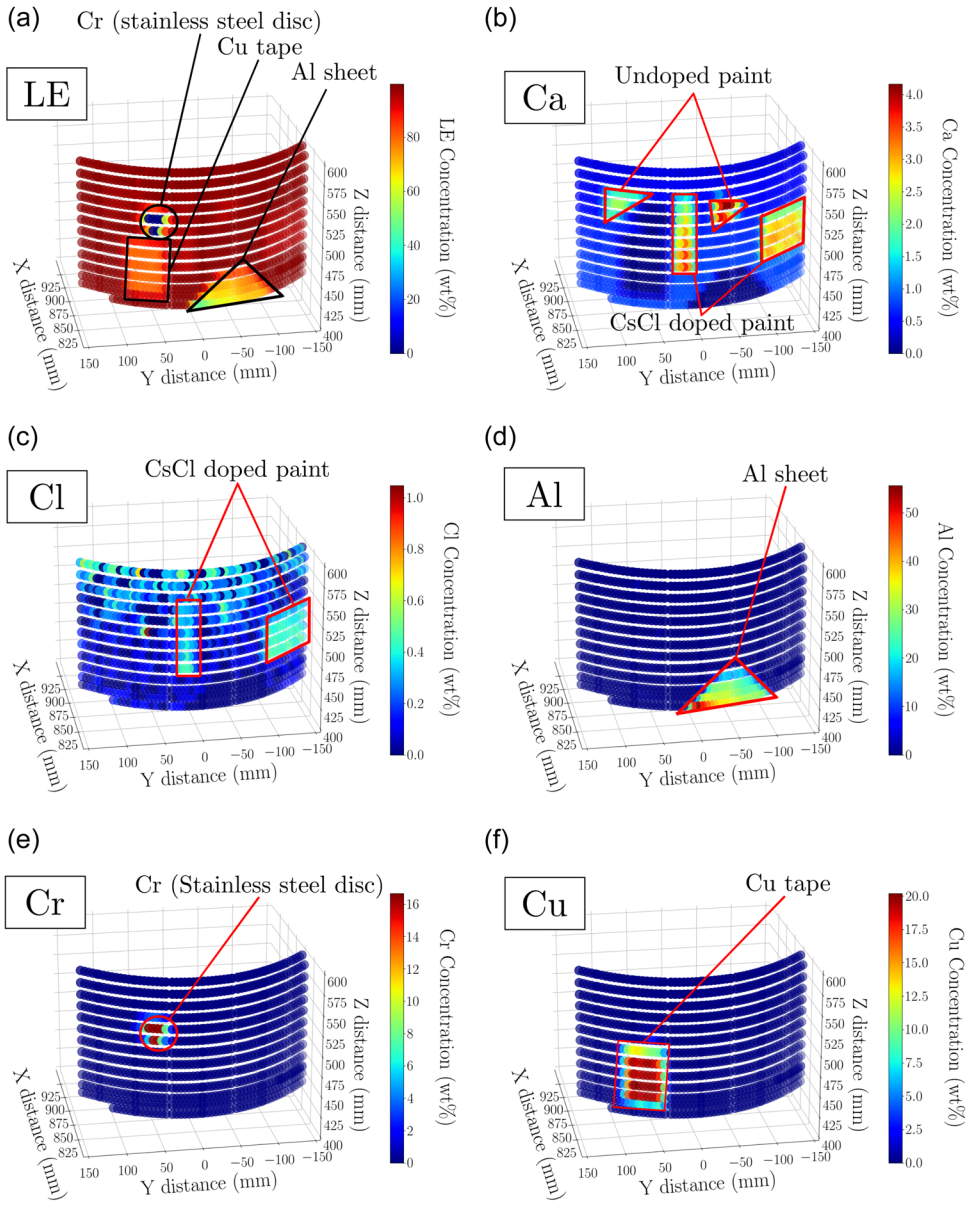

FIGURE 7 Three-dimensional surface concentration maps of the 200-L drum. (a) LE, (b) Ca (identifying the paint), (c) Cl (CsCl doped paint), (d) Al (identifying the aluminum sheet), (e) Cr (identifying the stainless steel), and (f) Cu (identifying the copper tape).

2 h, hence the surface was analyzed in a time-efficient process without sacrificing detail, as there remains a high point density on the objects of interest. To attain this level of detail using a basic surface scan would take in excess of 8 h, more than four times as long. Such an optimized system has tremendous applicability to the sorting and segregation of mixed nuclear wastes, enabling objects to be identified in terms of material composition. It is envisaged that this will be used as a complementary tool alongside gamma spectroscopy and LRS, to provide in situ material characterization. This means objects can be sorted with confidence, thereby reducing the risk of undesirable waste evolution during long-term disposal.

3.3 | Drum surface scanning

The ED-XRF maps of the drum surface are shown in Figure 7, with the element of interest and concentration in mass fraction (wt%) presented for Light Elements (LE), calcium (Ca), chlorine (Cl), aluminum (Al), chromium (Cr), and copper (Cu) for Figure 7a–f, respectively.

Figure 7 shows the robotic ED-XRF mapping system successfully located and identified the elements adhered to the drum's surface. Ca is naturally present in the paint, with the painted shapes clearly identifiable on the Ca map of Figure 7b. The CsCl, which was

dissolved into the paint, can also be observed in the Cl map of Figure 7c. It should be noted that additional Cl spots can be seen within this figure, likely a result of sweat from fingertips being deposited on the drum surface during the experimental setup. The metallic objects are also clearly identifiable in Figure 7d–f, demonstrating the ED-XRF's capability to accurately determine metals. The ability to scan a drum surface shows how XRF mapping can be achieved outside of regular 2D surface scanning. This has many potential applications, including routine in situ drum scanning in waste stores where it is crucial to identify and remove aggressive species on the drum's exterior, thereby preventing localized corrosion.

4 | CONCLUSIONS AND FUTURE WORK

Following the comparatively recent developments in ED-XRF systems, such platforms have been almost exclusively used for discrete hand-held single-point compositional analysis, undertaken by human operators. This study has shown the successful application of miniaturized ED-XRF to undertake efficient, robotically automated elemental analysis across a range of nuclear-applicable scenarios, as part of a robotic system, comprising a KUKA LBR iiwa and Olympus Vanta ED-XRF. The robotic ED-XRF system has a demonstrable capability to perform point mapping across flat surfaces, over meter-scale lengths. A system calibration was completed to test the accuracy of the ED-XRF device, showing a limited capability to recover the relative concentration of Cl in multiple paint samples collected on a strip. However, crucially, the system demonstrated a capability to detect the presence of elements, which was the primary objective of this study. The dynamic nature of the robotic manipulator's orientation control facilitates XRF mapping on more complex 3D surfaces, as demonstrated through the XRF mapping on the curved surface of a 200-L drum. The system was able to discern five different elements on the surface, displaying the results in 3D with custom-designed visualization software. Robotic manipulator systems are versatile platforms, which can take advantage of sensory technology. In this case an Intel® RealSense™ L515 depth camera was used, to enable 3D object data capture, thereby exhibiting a degree of intelligence in targeted mapping for enhanced assay, through identifying objects on a surface and subsequently characterizing them. The system demonstrated here was able to autonomously identify and characterize different objects in a time-efficient manner.

The robotic ED-XRF system presented in this study is highly applicable to a number of different applications, owing to the versatility of the scanning methodologies. Surface scanning could be applied to historical artifacts for XRF analysis, or used in a nuclear or other industrial settings for routine monitoring of objects and surfaces searching for contamination. Such a scanning methodology for the identification of contaminants could be combined with a decontamination procedure, such as pressure washing or swabbing, to provide a time and resource-efficient solution without placing humans in danger. The vision-based scanning of target objects is highly applicable to the sorting and segregating of mixed nuclear wastes to ensure correct characterization and consignment for storage and disposal. In such a setting, this would be particularly powerful as a complementary characterization tool in combination with gamma spectroscopy and LRS. Together these in situ analysis techniques would be capable of identifying a full spectrum of chemicals, materials, and compounds. Similar systems are desired for waste electronics recycling, so it is easy to see how the vision-based scanning methodology could be reapplied for use in other applications.

ACKNOWLEDGMENTS

We acknowledge the support of the University of Bristol National Nuclear User Facility (NNUF) for Hot Robotics, funded by BEIS and EPSRC. In particular Sabrina Shirazi for her assistance with hiring the KUKA LBR and Olympus Vanta systems. We would also like to thank James Parker at Olympus Corporation, for his support with the XRF system. Bartosz Dworzanski for his valuable technical support. Jim Brooke, DRPS for the School of Physics, for his assistance in ensuring the XRF system was robotically deployed safely during this study. The UK Research and Innovation with funding from the Engineering and Physical Sciences Research Council (EPSRC) towards the Robotics and AI in Nuclear (RAIN) research hub (EP/R026084/1), the National Centre for Nuclear Robotics (NCNR) (EP/R02572X/1), and the National Nuclear User Facility for Hot Robotics (EP/T011491/1).

CONFLICTS OF INTEREST

The authors declare no conflicts of interest.

ORCID

Samuel R. White http://orcid.org/0000-0001-6041-1205

REFERENCES

Allwood, A.C., Hurowitz, J.A., Clark, B.C., Cinquini, L., Davidoff, S., Denise, R.W. et al. (2021) The PIXL instrument on the mars 2020 perseverance rover. *Lunar and Planetary Science Conference*, 52, p.2. Available from: https://doi.org/10.48550/ARXIV.2103.07001

Balasubramanian, G. & Muthukumaraswamy, S.A. (2016) Element analysis with fundamental parameters using an XRF spectrum analysis matlab algorithm. *International Journal of Engineering and Applied Sciences (IJEAS)*, 3, 4.

Callcott, T.A. (1999) 13-Soft X-ray fluorescence spectroscopy. In: Ederer, D. (Ed.) *Vacuum ultraviolet spectroscopy*. Burlington: Academic Press, pp. 279–300. Available from: https://doi.org/10.1016/B978-012617560-8/50035-9

Campos, P., Appoloni, C., Rizzutto, M., Leite, A., Assis, R., Santos, H. et al. (2019) A low-cost portable system for elemental mapping by XRF aiming in situ analyses. *Applied Radiation and Isotopes*, 152, 78–85. Available from: https://doi.org/10.1016/j.apradiso.2019.06.018

Coffey, P., Smith, N., Lennox, B., Kijne, G., Bowen, B., Davis-Johnston, A. et al. (2021) Robotic arm material characterisation using LIBS and Raman in a nuclear hot cell decommissioning environment. *Journal of Hazardous Materials*, 412, 125193. Available from: https://doi.org/10.1016/j.jhazmat.2021.125193

Cremersand, D. & Radziemski, L. (2006) *Handbook of laser-induced breakdown spectroscopy*. Chichester, England: Wiley.

Croudace, I.W., Löwemark, L., Tjallingii, R. & Zolitschka, B. (2019) High resolution XRF core scanners: a key tool for the environmental and palaeoclimate sciences [Advances in data quantification and application of high resolution XRF core scanners]. *Quaternary International*, 514, 1–4. Available from: https://doi.org/10.1016/j.quaint.2019.05.038

Design, N.D.A.G.D.G.D.F. (2016) *Reological disposal generic disposal facility design*. Nuclear Decommissioning Authority. Tech. Rep. Available from: https://assets.publishing.service.gov.uk/government/uploads/system/uploads/attachment_data/file/635113/NDA_Report_no_DSSC-412-01_-_Geological_Disposal_-_Generic_Disposal_Facility_Designs.pdf [Accessed 18-02-2021].

FANUC: robotics in food processing. (2021) Available from: https://www.fanuc.eu/uk/en/customer-cases/foodprocessing-robot [Accessed 25-01-2021].

Fujiwara, K., Tani, J., Hironaga, M. & Tanaka, Y. (2017) Corrosion behaviour of aluminium under simulated environmental conditions of low-level waste. *Corrosion Engineering, Science and Technology*, 52(suppl 1), 162–165. Available from: https://doi.org/10.1080/1478422X.2017.1306390

Girão, A., Caputo, G. & Ferro, M. (2017) Application of scanning electron microscopy-energy dispersive X-ray spectroscopy (SEM-EDS). Comprehensive Analytical Chemistry, 75, 153–168. Available from: https://doi.org/10.1016/bs.coac.2016.10.002

Godfrey, L.V. & Glass, J.B. (2011) Chapter twenty-two—the geochemical record of the ancient nitrogen cycle, nitrogen isotopes, and metal cofactors. In: Klotz, M.G. (Ed.) *Research on nitrification and related processes, part a*. Academic Press, pp. 483–506. Available from: https://doi.org/10.1016/B978-0-12-381294-0.00022-5

Intel®RealSense l515 specifications. (2021) Available from: https://www.intelrealsense.com/lidar-camera-l515/ [Accessed 10-10-2021].

Janssens, K., Alfeld, M., Van der Snickt, G., De Nolf, W., Vanmeert, F., Radepont, M. et al. (2013) The use of synchrotron radiation for the characterization of artists' pigments and paintings. *Annual Review of Analytical Chemistry*, 6(1), 399–425. Available from: https://doi.org/10.1146/annurev-anchem-062012-092702

Janssens, K., Vittiglio, G., Deraedt, I., Aerts, A., Vekemans, B., Vincze, L. et al. (2000) Use of microscopic XRF for non-destructive analysis in art and archaeometry. *X-Ray Spectrometry*, 29(1), 73–91. Available from: https://doi.org/10.1002/(SICI)1097-4539(200001/02)29:13.0.CO;2-M

Kim, G.B., Boyd, S.T.P., Cantor, R.H., Bernstein, L.A. & Friedrich, S. (Eds.) (2019) A new measurement of the 60 keV emission from Am-241 using metallic magnetic calorimeters. In: 18th International workshop on low temperature detectors. New York, USA: Springer.

KUKA LBR iiwa. (2021) Available from: https://www.kuka.com/en-gb/products/robotics-systems/industrial-robots/lbr-iiwa [Accessed 10-02-2021].

Longoni, A., Fiorini, C., Leutenegger, P., Sciuti, S., Fronterotta, G., Strüder, L. et al. (1998) A portable XRF spectrometer for non-destructive analyses in archaeometry. *Nuclear Instruments and Methods in Physics Research Section A: Accelerators, Spectrometers, Detectors and Associated Equipment*, 409(1), 407–409. Available from: https://doi.org/10.1016/S0168-9002(98)00113-2

Malvern Panalytical. (2020) *Malvern Panalytical Zetium Datasheet*. Available from: https://www.malvernpanalytical.com/en/products/product-range/zetium [Accessed 2020-12-10].

Muhammed Shameem, K., Dhanada, V., Harikrishnan, S., George, S.D., Kartha, V., Santhosh, C. et al. (2020) Echelle LIBS-Raman system: a versatile tool for mineralogical and archaeological applications. *Talanta*, 208, 120482. Available from: https://doi.org/10.1016/j.talanta.2019.120482

Nuclear Decommissioning Authority. (2008) *Waste package specification and guidance documentation: WPS/640: guidance on the monitoring of waste packages during storage*. Tech. Rep. Available from: https://assets.publishing.service.gov.uk/government/uploads/system/uploads/attachment_data/file/876828/WPS- [Accessed 17-12-2020].

Nuclear Decommissioning Authority. (2012) *Industry guidance interim storage of higher activity waste packages—integrated approach*. Tech. Rep. Available from: https://cumbria.gov.uk/elibrary/Content/Internet/538/755/1929/17716/17718/41338115617.PDF [Accessed 19-10-2021].

Nuclear Decommissioning Authority. (2016) *Geological disposal waste package evolution status report*. Tech. Rep. Available from: https://rwm.nda.gov.uk/publication/geological-disposal-waste-package-evolution-status-report/ [Accessed 06-01-2021].

Nuclear Decommissioning Authority. (2019) *Nuclear Decommissioning Authority: radioactive waste strategy*. Tech. Rep. Available from: https://assets.publishing.service.gov.uk/government/uploads/system/uploads/attachment_data/file/838828/Radioactive_Waste_Strategy_September_2019.pdf [Accessed 19-10-2021].

Nuclear Decommissioning Authority. (2020) *Waste package specification and guidance documentation: specification for waste packages containing low heat generating waste: part c—fundamental requirements*. Tech. Rep. Available from: https://assets.publishing.service.gov.uk/government/uploads/system/uploads/attachment_data/file/935717/WPS_220_01_Part_C_-_Specification_for_Waste_Packages_Containing_Low_Heat_Generating_Waste.pdf

Olympus Vanta specifications. (2021) *Olympus Corporation*. Available from: https://www.olympus-ims.com/en/vanta/ [Accessed 25-01-2021].

Sellafield Ltd. (2020) *Sort and segregate nuclear waste: specification*. Available from: https://www.gov.uk/government/publications/sort-and-segregate-nuclear-waste-specification/sort-and-segregate-nuclear-waste-specification [Accessed 21-12-2020].

Streli, C., Wobrauschek, P. & Kregsamer, P. (1999) X-ray fluorescence spectroscopy, applications. In: Lindon, J.C. (Ed.) *Encyclopedia of spectroscopy and spectrometry*. Oxford: Elsevier, pp. 2478–2487. Available from: https://doi.org/10.1006/rwsp.2000.0337

Thomas Renner. (2021) Tech briefs: Robots bring airplane production up to speed. Available from: https://www.techbriefs.com/component/content/article/tb/supplements/md/features/applications/33714 [Accessed 25-01-2021].

Thomsen, V. & Schatzlein, D. (2002) Advances in field-portable XRF. *Spectroscopy—Springfield then Eugene then Duluth*, 17.

Turner, A. (2017) In situ elemental characterisation of marine microplastics by portable XRF. *Marine Pollution Bulletin*, 124(1), 286–291. Available from: https://doi.org/10.1016/j.marpolbul.2017.07.045

Turner, A., Poon, H., Taylor, A. & Brown, M.T. (2017) In situ determination of trace elements in Fucus spp. by field-portable-XRF. *Science of the Total Environment*, 593–594, 227–235. Available from: https://doi.org/10.1016/j.scitotenv.2017.03.091

Turner, A. & Taylor, A. (2018) On site determination of trace metals in estuarine sediments by field-portable-XRF. *Talanta*, 190, 498–506. Available from: https://doi.org/10.3389/frobt.2020.499056

White, S.R., Megson-Smith, D.A., Zhang, K., Connor, D.T., Martin, P.G., Hutson, C. et al. (2020) Radiation mapping and laser profiling using a robotic manipulator. *Frontiers in Robotics and AI*, 7, 141. Available from: https://doi.org/10.3389/frobt.2020.499056

Wilkinson, K., Lundkvist, J., Seisenbaeva, G. & Kessler, V. (2011) New tabletop SEM-EDS-based approach for cost-efficient monitoring of airborne particulate matter. *Environmental Pollution*, 159(1), 311–318. Available from: https://doi.org/10.1016/j.envpol.2010.08.024

Wilschefski, S.C. & Baxter, M.R. (2019) Inductively coupled plasma mass spectrometry: introduction to analytical aspects [cbr-40-115[PII]]. The clinical biochemist. *Reviews*, 40(3), 115–133.

Wilson, P. (Ed.) (1996) *The nuclear fuel cycle from ore to waste*. New York, USA: Oxford Science Publications.

Zieba-Palus, J., Borusiewicz, R. & Kunicki, M. (2008) Praxis-combined-Raman and -XRF spectrometers in the examination of forensic samples. *Forensic Science International*, 175(1), 1–10. Available from: https://doi.org/10.1016/j.envpol.2010.08.024

How to cite this article: White, S.R., Mrtin, P.G., Megson-Smith, D.A. & Scott, T.B. (2022) Application of automated and robotically deployed in situ X-ray fluorescence analysis for nuclear waste management. *Journal of Field Robotics*, 39, 1205–1217. https://doi.org/10.1002/rob.22104